Synthesis and Characterizations of Membrane Composite Polymer Liquid Crystal of PMMA-RM257-Doped with Lithium Ions

Afrizal Afrizal[1*], Setia Budi[1], Asep Riswoko[2], Teguh Budi Prayitno[3], and Della Dewanda[1]

[1]*Department of Chemistry, Faculty of Mathematics and Natural Sciences, Universitas Negeri Jakarta, Jl. Rawamangun Muka No. 10, Jakarta Timur 13220, Indonesia*

[2]*Research Center for Polymer Technology – National Research and Innovation Agency (BRIN), KST BJ Habibie, Kawasan Puspiptek Building 460, Tangerang Selatan 15314, Indonesia*

[3]*Department of Physics, Faculty of Mathematics and Natural Sciences, Universitas Negeri Jakarta, Jl. Rawamangun Muka No. 10, Jakarta Timur 13220, Indonesia*

* ***Corresponding author:***

tel: +62-81314484533
email: afrizal@unj.ac.id

Received: May 15, 2025
Accepted: October 29, 2025

DOI: 10.22146/ijc.106762

Abstract: *A membrane composite polymer liquid crystal of polymethyl methacrylate with mesogen reactive 257, doped with lithium ions (PMMA-RM257-Li), has been successfully synthesized. Synthesized PMMA-RM257-Li using methods of UV exposure to polymer solutions and were made with RM257 variations of 10, 30, 50, 70 and 90 wt.%. Membrane composite polymer PMMA-RM257-Li was characterized by FTIR where absorption peaks appear at wavenumbers 2935 cm^{-1} indicating the-CH_3 group, 1730 cm^{-1} indicating the C=O group, and 1630–1660 cm^{-1} indicating the presence of aromatic groups. XRD analysis results showed that the membrane polymer PMMA-RM257-Li is semicrystalline. The composite membrane obtained optimum test results at the addition of 50 wt.% RM257 with an ionic conductivity of 1.01 × 10^{-3} S/cm and an ion exchange capacity value of 0.02385 meq/g. This study shows that the addition of 50 wt.% RM257 provides the most optimal membrane characteristic results. The characterization results showed that the addition of lithium ions to the manufacture of PMMA-RM257 membranes improved the membrane's capabilities for membrane fuel cell technology.*

Keywords: *methyl methacrylate; membrane; reactive mesogen; conductivity*

■ INTRODUCTION

Membrane composite polymer is a material that is made from more than one monomer or a combination of monomers and other materials. The advantage of membrane materials made from a combination of more than one material is the combination of the strengths of each of these materials. So, it is expected that the resulting membrane will have some advantages. Research on membranes has been growing significantly today, particularly in the field of polymer electrolyte membranes used in fuel cell technology. The material for making the membrane greatly affects the results of the membrane. In several studies, it is reported that the PEM membrane used is fluorinated membranes or the perfluorosulfonic acid (PFSA) polymers known as Nafion membranes. However, Nafion's membrane has some drawbacks including a decrease in ionic conductivity and low humidity at high temperatures. For these reasons, other proton-conducting membranes was made in this research. Therefore, an in-depth study of the materials to make the membrane is needed [1-3].

Polymethyl methacrylate (PMMA) is an essential and interesting polymer because of its attractive optical and physical characteristics decisive about its area applications. It is a transparent polymer that has high durability, weather resistance and a high refractive index. However, the use of pure PMMA has limited mechanical properties, is less compatible, rigid and non-bioactive. One way that can be done is to combine PMMA with reactive mesogens. Polymers combined with reactive mesogens will form a liquid crystal polymer network,

resulting in more robust mechanical properties. Reactive mesogen RM257 is one of the monomer liquid crystals that was polymerized by photopolymerization [4-5].

One of the important factors in a polymer composite membrane is its conductivity. Therefore, to improve the conductivity properties of the membrane composite, in this study, the PMMA-RM257 membrane was added lithium acetate (CH_3COOLi). Research conducted by other researchers showed results that the addition of CH_3COOLi salts to the PMMA/CH_3COOLi solid membrane can increase ionic conductivity to the optimum of 8.21×10^{-5} S/cm at a 60:40 variation. In addition, CH_3COOLi was chosen because of its relatively affordable price compared to some other lithium salts, such as LiTFSI and LiBOB and has a high solubility level in most solvents, especially polar organic solvents such as DMF [6-7].

One type of membrane that is currently being developed is a polymer membrane for fuel cell systems. The problem in the previous study is that the conductivity value of the membrane that has been widely used is still low for a PEM membrane. The combination of PMMA with reactive mesogen RM257 and the presence of lithium-ion doping is expected to increase the conductivity value and ion exchange capacity. The reactive mesogen RM257, in some studies, has good conductivity values, especially with the addition of lithium ions. Therefore, in this article, it is reported that the results of research on the manufacture of PMMA-RM257-Li polymer membrane have great potential for becoming a polymer membrane in the fuel cell system. The use of RM257 is due to the ability of its monomers to be polymerized and also exhibit liquid crystallinity, which is expected to play a role in the fuel cell process. Combining the capabilities of PMMA and RM257 is the idea reported in this article. The results are expected to provide opportunities to become membrane fuel cells [8-10].

The polymer composite membrane produced from this research is expected to be an alternative to the fuel cell membrane that has been used so far. The results of previous research show that PMMA-RM257 a polymer composite membrane that has the opportunity to be used as a fuel cell membrane. This is based on the chemistry and chemistry of the membrane, especially its ability as an electrolyte polymer membrane [11-12]. Synthesis of membrane composite polymer liquid crystal PMMA-RM257-Li made in this study using methods of UV exposure to polymer solutions. Membrane polymer solutions were made with variations in RM257 of 10, 30, 50, 70, and 90 wt.%. The liquid crystals of RM257 are made in variations with the aim of analyzing how the composite polymer membranes are produced. Membrane characterization is polarizations optics microscope (POM), Fourier transformed infrared (FTIR), scanning electron microscopy (SEM), and X-ray diffraction (XRD). Membrane composite of PMMA-RM257-Li was tested for ionic conductivity and ion exchange capacity (IEC).

■ EXPERIMENTAL SECTION

Materials

The materials used are methyl methacrylate (MMA), dimethylformamide (DMF), chloroform, benzoyl peroxide (BPO), and reactive mesogen RM257.

Instrumentation

The tools used in this research are 25 W UV lamp, spatula, analytical balance, magnetic stirrer, hotplate stirrer, aluminum, black box, drop pipette, thermometer, and beaker. FTIR ALPHA II BRUKER was used to determine the functional groups in the membrane composite PMMA-RM257-Lithium. Morphology surface of membrane composite PMMA-RM257-LI was studied using SEM-EDX Zeiss EVO MA10, where the data obtained from SEM produces a three-dimensional micrograph in the form of images. XRD Empyrean Series 3 (Malvern PANalytical, UK) was used to determine the crystalline nature of the sample. This analysis will bring up specific peaks.

Procedure

The manufacture of PMMA-RM257-Li membrane begins with the process of mixing MMA monomers with RM257 monomers and CH_3COOLi 40 wt.% in DMF and chloroform solvents. The dissolution was carried out in a glass beaker at room temperature and a 20 wt.%

solution was produced. The same was done for RM257 by making solutions with variations of 10, 30, 50, 70 and 90 wt.%. After that, the MMA solution was mixed with the RM257 solution in a 1:1 ratio. BPO initiator as much as the tip of a spatula was added to the MMA-RM257 mixture at 95 °C within 5 min and a speed of 250 rpm. Then the MMA-RM257 sample was poured onto a Printed Circuit Board coated with copper electrodes with an interdigital structure and then polymerized using the UV curing method for 15 min. Composite membrane manufacturing by making a 60 wt.% MMA solution in DMF. Furthermore, solutions of CH_3COOLi at 40 wt.% and RM257 with variations of 10, 30, 50, 70, and 90 wt.% are made in the same way. Each solution is then mixed in equal proportions and homogenized at 600 rpm for 6 h at 40–45 °C. Next, samples were added to the BPO initiator and then homogenized at room temperature at 250 rpm for 5 min.

■ RESULTS AND DISCUSSION

Membrane PMMA-RM257-Li was made by the process of photopolymerization of MMA with RM257 using the UV curing method. Polymerization begins with the initiation stage, where the addition of BPO will break the double bond (addition) on MMA and RM257 to form free radicals between MMA and RM257 [13-15]. In the second stage, i.e., the propagation stage, PMMA and RM257 free radicals form a continuous cross-linked polymer chain. The use of UV light will direct the end groups on the RM257 and MMA monomers to form a liquid crystal polymer network, furthermore, after the molecule stabilizes, there will be a cessation of polymer chain growth, which is the termination stage. The cross-link that occurs between MMA-RM257 is a covalent bond predicted to have a reaction mechanism as shown in Fig. 1.

Liquid crystalline polymers have distinctive properties of their texture, which are shown from the texture patterns observed using a POM. Based on Fig. 2, the texture of the liquid crystal on the PMMA-RM257-Li polymer composite membrane can be seen to be evenly textured in each variation of the RM257 composition [16-18]. The composition of RM257 30 and 70 wt.% has a separate droplet texture that has a different color on each droplet and is neatly arranged, which is a characteristic of liquid crystal polymers. At the time of

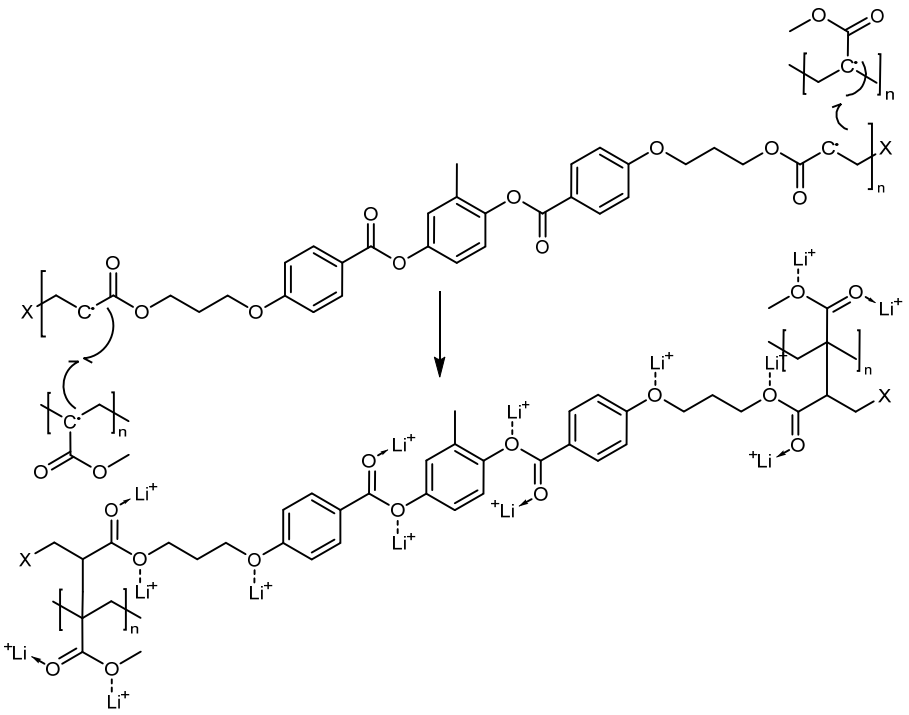

Fig 1. Polymerization structure scheme of PMMA-RM257-Li

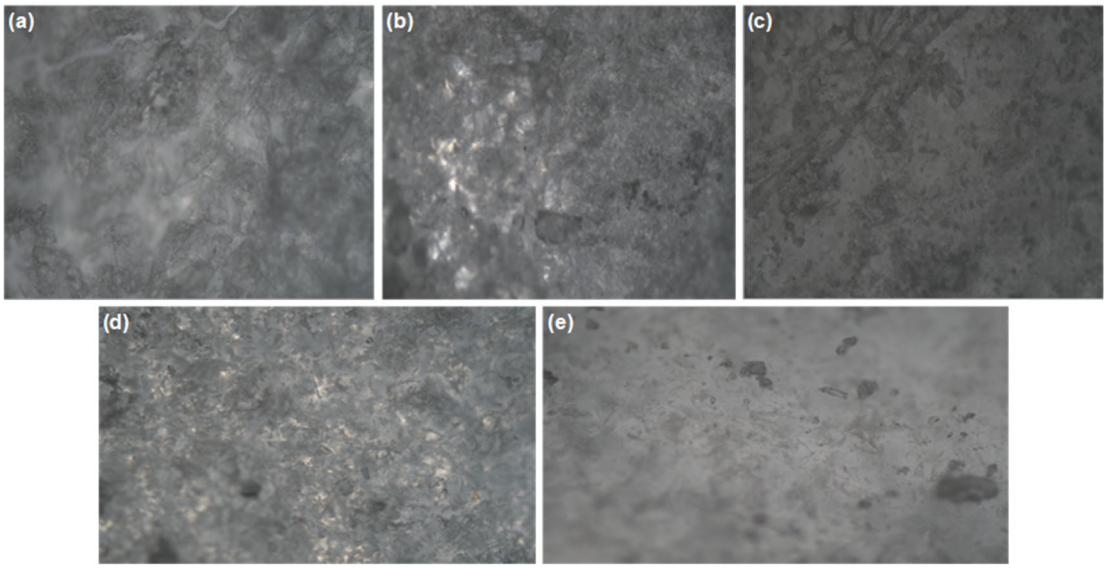

Fig 2. POM textures membrane composite of PMMA-RM257-Li with variations: (a) 10, (b) 30, (c) 50, (d) 70, and (e) 90 wt.% of RM257

the composition of RM257, as much as 30 wt.%, there was a change in texture, which was originally the texture of the droplet, evenly changed to a change in certain parts to form an aggregate [19-20]. This suggests the possibility of polymerization, which forms elastomers in certain areas. However, there is still the original separated droplet. Therefore, it can be concluded that when the composition of RM257 is 30 and 70 wt.%, a suitable PMMA-RM257-Li polymer composite membrane is produced.

The results of the surface texture observation of the PMMA-RM257-Li composite polymer membrane can be confirmed by SEM analysis (Fig. 3). Based on the results, the photo SEM of membrane composite polymer PMMA-RM257-Li at all compositions, ranging from 10 to 90 wt.% RM257 showed a layered morphology on the surface of membrane, which is not smooth, suggesting agglomeration (clumping). The membrane composite polymer at 50 wt.% RM257 shows surface membrane morphology, smooth and there are molecular shapes of bars with close proximity. In some parts, there is agglomeration (clumping) where there are shapes like bars, which are characteristic of reactive mesogens. The sample with 50 wt.% RM257 variation gives good smoothness and uniformity results, which indicate that RM257 and lithium ion have filled the cavity in the PMMA matrix perfectly [21-23].

Based on Fig. 4, the spectra of the three samples with varying mass percentages of RM257 have a shape that is

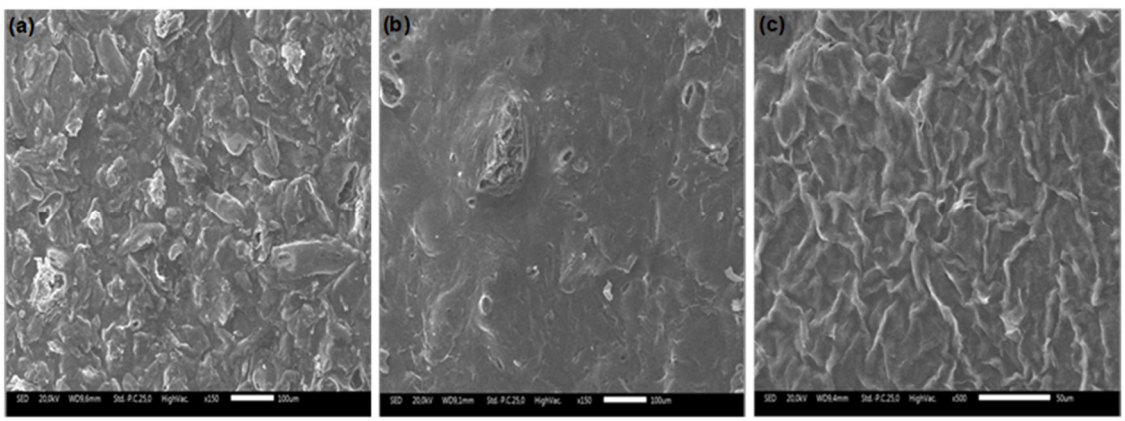

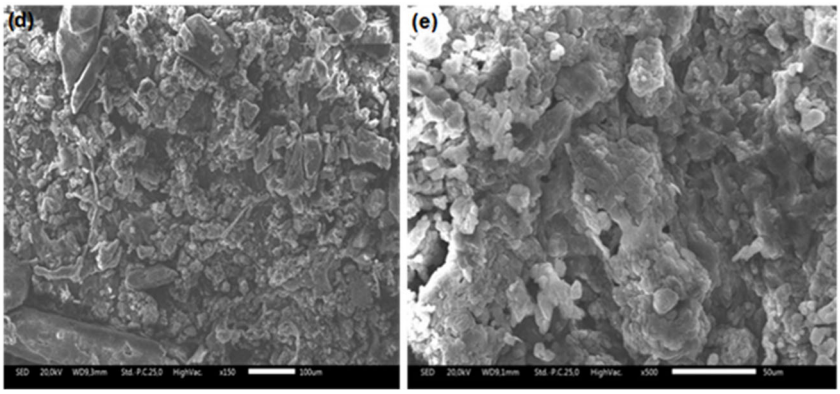

Fig 3. SEM images of PMMA-RM 257-Li: (a) 10, (b) 30, (c) 50, (d) 70, and (e) 90 wt.%

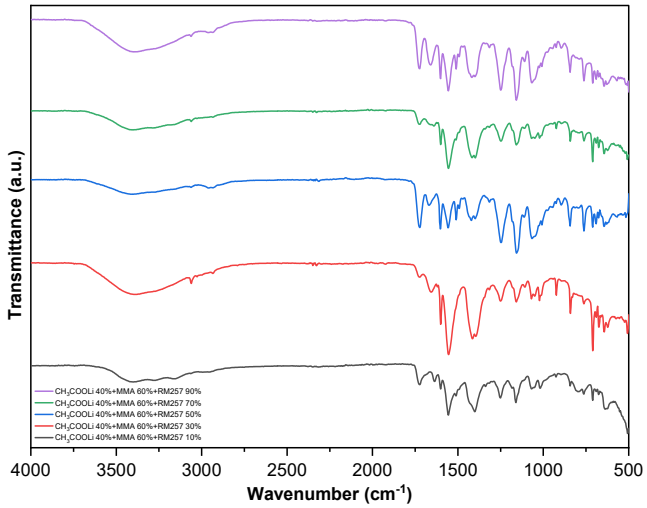

Fig 4. FTIR spectra of membrane composite polymer PMMA-RM257-Li

not much different. There is a wide peak indicating the presence of an elongated vibration O–H group at 3394 cm^{-1}. There is a peak with low intensity, indicating the presence of $–CH_3$ group with asymmetric strain vibration type at 2935 cm^{-1}. The peak of 1730 cm^{-1} shows the presence of C=O bonds, indicating the presence of ester functional groups in the sample with the type of stretch vibration. The absorption peak of 1602 cm^{-1} indicates the presence of aromatic groups belonging to RM257. An absorption peak at 1248 cm^{-1} indicating the presence of C–O–C bonds stretching vibrations in ether groups in both PMMA and RM257 structures, and at 1060–1144 cm^{-1} an absorption peak appears, indicating the presence of C–O bonds with stretching vibrations. Due to the discovery of the C–O functional group, it can be concluded that this compound is an ester [24-25].

At 1670 cm^{-1}, no absorption peak appeared indicating the absence of the C=C group, which in the MMA structure displays an absorption peak at this wavenumber. In addition, in this spectrum there is no absorption peak at 3100 cm^{-1}, indicating the absence of $=CH_2$ (vinyl) groups belonging to MMA. This difference in structural characteristics indicates that the MMA and RM257 monomers have bonded by forming covalent bonds. In the three spectra above, the peak intensity increases slightly as the mass percentage of RM257 increases, which explains that the concentration of RM257 affects the intensity of the PMMA-RM257-Li infrared spectrum.

At 1600 cm^{-1} there is an absorption peak indicating the presence of C=C aromatic, a special longitudinal vibration of RM257. The peak of absorption that appears at 1557 cm^{-1} with high intensity indicates the presence of a COO-group of elongated vibration and the peak at 1250 cm^{-1} indicates the presence of a C–O bond of elongated vibration ester. There is an absorption peak at 1021 cm^{-1}, which indicates the presence of a Li–O bond with elongated vibrations. In the fingerprint area, there are peaks in 761–763 and 841–843 cm^{-1}, C–H is substituted 1,2 (*ortho*) and C–H is substituted 1,4 (*para*). According to previous research, the effect of the presence of lithium salts will result in the coordination of salt cations in polar groups in the polymer matrix [26-27].

PMMA has a peak width at $2\theta = 13.20°$, 31° and 35° indicating the amorphous structure. The membrane PMMA-RM257-Li showed a sharp peak at $2\theta = 16.33°$, 24.02°, 44.68°, and 72.54°, which indicates crystalline

properties. For the membrane with a variation of 50 wt.% RM257, there is a wide peak at 2θ = 20.82°, while in the variation of 70 and 90 wt.% RM257 there is a wide peak at 2θ = 20.5°. Along with the increase in the concentration of RM257, it was observed that the peak at 2θ = 31° disappeared. The loss of this peak indicates that the increased concentration of RM257 makes the properties of the membrane semi-crystalline. While CH_3COOLi has crystalline properties that have a sharp peak at 2θ = 7.7°, 10.1°, 21.1°, 26.1°, and 30.9° [28].

While some other peaks are less sharp, this identifies the presence of a semicrystalline phase in the membrane produced. In Fig. 5, the diffraction pattern at variations of 10 and 30 wt.% RM257 shows crystalline properties characterized by the presence of sharp peaks, while in variations of 50, 70, and 90 wt.% RM257 shows semi-crystalline properties characterized by wide and sharp peaks. At variations of 10 and 30 wt.% RM257, no typical width peak of PMMA was found at 2θ = 13.20°, 31°, and 35°. However, in the diffraction pattern, there are peaks with high intensity at 2θ = 44.9° and peaks with moderate to low intensity in the range of 2θ = 11–50.9°, which show crystalline properties. This crystalline phase comes from the orderly chain structure of the RM257 polymer, because the formed RM257 liquid crystalline polymer will have an orderly polymer chain orientation after the polymerization process. In this condition, the polymer chain fixation process of the LC RM257 polymer occurred [29-31]. This crystalline phase is expected to function when used as a membrane in fuel cell systems, where the process of releasing and capturing electrons occurs. So, based on the results of this XRD, it can be concluded that this research has succeeded in creating a membrane that can be an opportunity as a polyelectrified membrane (PEM) in the fuel cell system later [32-33].

The synthesized lithium-ion-doped PMMA/RM257 composite membrane was then tested for ion exchange capacity to determine the composite membrane's ability to exchange cations. The test was carried out by soaking the membrane in sulfuric acid for 24 h with the aim of protonating the composite membrane. After that, the membrane is washed with aqua DM so that the excess H^+ ions can be removed. The membrane is re-soaked with NaCl to exchange H^+ for Na^+ ions. The number of ions exchanged can be determined by titration using NaOH. The IEC value of composite membranes increases as the concentration of RM257, as shown in Fig. 6. However, it decreased when the concentration of RM257 was above 50 wt.%. The value of the ion exchange capacity at the addition of 10 wt.% RM257 is 0.00967 meq/g and at the addition of 30 wt.% RM257 is 0.01931 meq/g. In addition to 50 wt.% RM57, an IEC value of 0.02385 meq/g was obtained. The addition of 70 and 90 wt.% RM257 yielded IEC values of 0.01142 and 0.01166 meq/g. The magnitude of the IEC value represents the number of active sites or functional groups that play a role in the exchange of ions on the membrane. Based on this, the addition of 50 wt.%

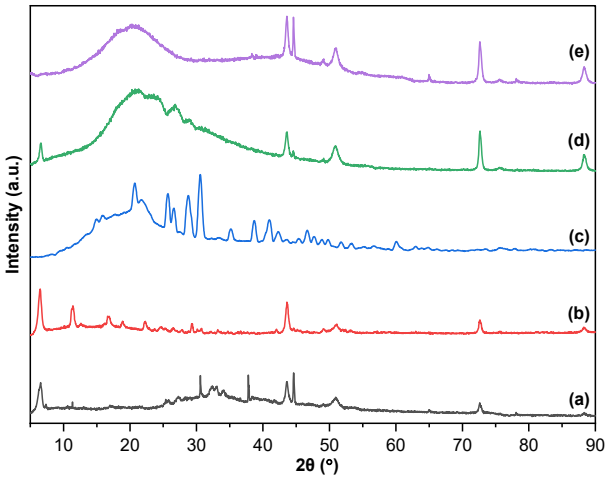

Fig 5. XRD of membrane PMMA-RM257-Li with a percentage weight variation of RM257: (a) 10, (b) 30, (c) 50, (d) 70, and (e) 90 wt.%

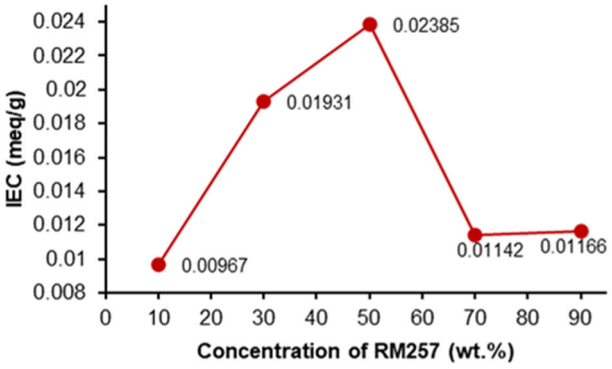

Fig 6. IEC graph of PMMA/RM257 composite membrane doped with lithium ion, with RM257 concentration variation

RM257 provides more ion exchange sites, allowing the composite membrane's ability to exchange ions to reach an optimal value of 0.02385 meq/g. Previous research has shown that an increase in IEC values will be in line with an increase in membrane conductivity [34-36].

The lithium ion-doped PMMA/RM257 composite membrane is measured for ionic conductivity using an LCR-meter that will produce a resistance value. Fig. 7 shows the conductivity values of composite membranes. At the addition of 10 and 30 wt.%, RM57 yielded ionic conductivity of 2.46×10^{-4} and 5.93×10^{-4} S/cm. At the addition of 50 wt.% RM257 yielded an ionic conductivity of 1.01×10^{-3} S/cm. The magnitude of the ionic conductivity of the membrane at the addition of 70 and 90 wt.% RM257 was 5.54×10^{-4} and 1.52×10^{-4} S/cm. Based on Fig. 6, there is an increase as the concentration of RM257 increases by reaching the optimal at an increase of 50 wt.% and then decreases when the concentration of RM257 is above 50 wt.% [37-38].

Conductivity was measured using the Sanwa LCR-700 type LCR meter. The capacitance value increases as the concentration of water vapor increases. Water vapor will settle in the cavity and surface space of the membrane. Water has a high dielectric constant; the diffusion of water vapor on the membrane increases the dielectric constant resulting in an increase in capacitance [39-40].

The capacitance value increases as the concentration of water vapor increases, as can be seen in Fig. 7. Water vapor will settle in the voids and surface space of the thin film. Water has a high dielectric constant; the diffusion of water vapor in the thin film increases the dielectric constant, which results in an increase in capacitance. The identification of the membrane composite of PMMA-RM257-Li is determined through the capacitance value, which explains how the composite membrane produced in this study is capable. This capacitance value represents the ability of composite membranes in subsequent applications.

Membrane composite polymer PMMA-RM257-Li, which consists of 40 and 30 wt.% RM257, shows better capacitance results, where high capacitance changes of up to 1700 pF are observed as RH increases. Whereas in the 20 wt.% RM257 sample, the change in capacitance is less

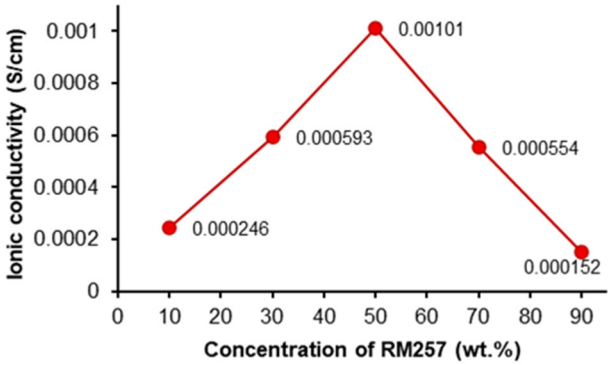

Fig 7. Graphic capacitance of membrane composite polymer of PMMA-RM257-lithium

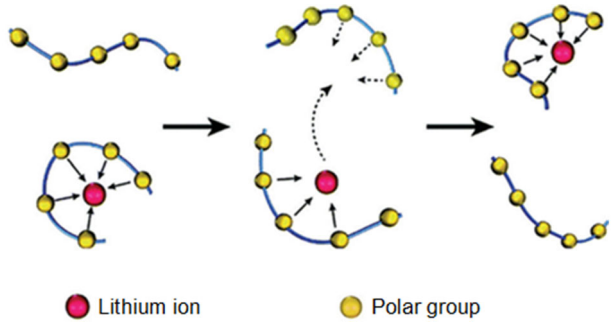

Fig 8. Mechanism of hopping pada membrane

than 100 pF. This could be due to the addition of RM257 concentration increasing the cluster grain size on the surface of the film, thus increasing the sensitivity of the film to the absorption of water molecules. The relationship between frequency and the change in capacitance is also evident, where a frequency of 1 kHz yields the greatest effect on the increase in capacitance in all samples.

Based on previous research, the decrease in ionic conductivity occurs due to a decrease in the segmental movement of polymers in the membrane, which can inhibit the mobility of ions so that the number of moving ions will be reduced. The highest ionic conductivity is owned by the membrane with an addition of 50 wt.% RM257, which is 1.01×10^{-3} S/cm. The possible mechanism of ion transfer in the membrane involves a hopping mechanism, also known as the Grotthuss mechanism (see Fig. 8). In this mechanism, the Li^+ ion will coordinate with the polymer's polar group during the segmental motion of the polymer, causing the Li ion to dissociate. Li ions that have been dissociated move

between sites by hopping in a polymer matrix. Thus, the existence of polar groups and segmental motion of polymers is an important factor to support more optimal ion transfer.

■ CONCLUSION

Membrane composite polymer PMMA-RM257-Li has been successfully made by the UV curing method. FTIR results show that MMA has polymerized into PMMA, where there is no 3100 cm^{-1} absorption, which is the vibration of the $-CH_2$ bond in the MMA spectrum. SEM results indicate that the PMMA-RM257-Li thin film with a 40 wt.% RM257 exhibits the best smoothness and uniformity. The value of the IEC at the addition of 10, 30, 50, 70, and 90 wt.% RM257 is 0.00967, 0.01931, 0.02385, 0.01142, and 0.01166 meq/g. At the addition of 10, 30, 50, 70, and 90 wt.% RM57 yielded ionic conductivity of 2.46×10^{-4}, 5.93×10^{-4}, 1.01×10^{-3}, 5.54×10^{-4}, and 1.52×10^{-4} S/cm. So that membrane composite of PMMA-RM257-Li that 30 and 40 wt.% RM257 variations have good electrical properties and sensitivity properties. The increase in RM257 concentration in the membrane composite shows differences in structure and electrical properties, where the greater the concentration, the better the structure and electrical properties of the sensor.

■ ACKNOWLEDGMENTS

The authors wish to thank Universitas Negeri Jakarta, Ministry of Education, Culture, Research, and Technology of the Republic of Indonesia, who financially supported this work through the research scheme *Penelitian Fundamental Reguler* under contract number 7/UN39.14/PG.02.00.PL/PFR/VI/2024 with the title research: *Kajian Sintesis Membran Komposit Mesogen Reaktif RM257-Polimer Metil Metakrilat Terdoping Ion Lithium dan Karakterisasi Sebagai Membran Polimer Elektrolit*.

■ CONFLICT OF INTEREST

There is no conflict of interest.

■ AUTHOR CONTRIBUTIONS

Afrizal, Setia Budi and Della Dewanda were responsible for collecting primary data, analyzing the data, visualizing the data, and interpreting the findings. Afrizal and Asep Riswoko drafted the initial manuscript, reviewed, and edited. Setia Budi and Teguh Budi Prayitno carried out formal analysis and supervision. Della Dewanda conducted supervision. Afrizal and Teguh Budi Prayitno was responsible for funding acquisition, methodology, supervision and approved the final version of the manuscript intended for publication.

■ REFERENCES

[1] Mu'izzah, N.R., Hapsari, P.Z., Aulia, N.P., Wulansari, D.W.T., Azhari, F., and Pramono, E., 2023, Utilization of lignin and lignosulfonate from oil palm empty fruit bunches as filler in PVDF proton exchange membrane fuel cell, *Indones. J. Chem.*, 23 (4), 1042–1053.

[2] Afrizal, A., Yusmaniar, Y., Valentino, B., Riswoko, A., and Khairunnisa Gumilar, K., 2024, Effect of methyl methacrylate concentrations on surface and thermal analysis of composite polymer polymethylmethacrylates with mesogen reactive RM82, *Des. Monomers Polym.*, 27 (1), 1–11.

[3] Göktaş, M., and Deng, G., 2018, Synthesis of poly(methyl methacrylate)-*b*-poly(*N*-isopropylacrylamide) block copolymer by redox polymerization and atom transfer radical polymerization, *Indones. J. Chem.*, 18 (3), 537–543.

[4] Mehrmashhadi, J., Wang, L., and Bobaru, F., 2019, Uncovering the dynamic fracture behavior of PMMA with peridynamics: The importance of softening at the crack tip, *Eng. Fract. Mech.*, 219, 106617.

[5] Nitti, F., Selan, O.T.E., Hoque, B., Tambaru, D., and Djunaidi, M.C., 2022, Improving the performance of polymer inclusion membranes in separation process using alternative base polymers: A review, *Indones. J. Chem.*, 22 (1), 284–302.

[6] Li, W., Chang, Z., Lin, Z., and Xu, X., 2020, Effect of montmorillonite on PEBAX®1074-based mixed matrix membranes to be used in humidifiers in proton exchange membrane fuel cells, *e-Polym.*, 20 (1), 171–184.

[7] Li, G., Zhu, D., Jia, W., and Zhang, F., 2021, Analysis of the aging mechanism and life evaluation of

elastomers in simulated proton exchange membrane fuel cell environments, *e-Polym.*, 21 (1), 921–929.

[8] Wrubbel, N., Ritter, H., Reuter, K., Karbach, A., and Drechsler, D., 2006, Annealing effects on the electrical conductivity of polymerized liquid crystalline 3,4-ethylenedioxythiophene derivatives, *e-Polym.*, 6 (1), 002.

[9] Hussein, A., Yousif, E., Rasheed, M., Ahmed, D., Bufaroosha, M., and Kadhom, M., 2025, Enhanced UV resistance of poly(methyl methacrylate) through Schiff base and metal oxide nanoparticle incorporation, *Indones. J. Chem.*, 25 (2), 348–358.

[10] Ngadiwiyana, N., Prasetya, N.B.A., Gunawan, G., Kusworo, T.D., and Susanto, H., 2021, Synthesis, characterization, and study of proton exchange polymer membrane properties of sulfonated copolymer eugenol-diallyl phthalate, *Indones. J. Chem.*, 21 (1), 168–178.

[11] Jiang, J., Qu, E., Xiao, M., Han, D., Wang, S., and Meng, Y., 2020, 3D Network structural poly (aryl ether ketone)-polybenzimidazole polymer for high-temperature proton exchange membrane fuel cells, *Adv. Polym. Technol.*, 2020, 4563860.

[12] Suen, M.C., Gu, J.H., Hwang, J.J., Wu, C.L., and Lee, H.T., 2018, *In-situ* polymerization and characteristic properties of the waterborne poly (siloxanes-urethane) s nanocomposites containing graphene, *J. Polym. Res.*, 25 (1), 33.

[13] Sant, S., and Klok, H.A., 2024, Linear, Y- and Ψ-shaped poly(2-(dimethylamino)ethyl methacrylate) and poly(methyl methacrylate) brushes prepared by surface-initiated polymerization from a homologous series of ATRP initiators, *Eur. Polym. J.*, 205, 112706.

[14] Al-Jumaili, M.H.A., Hamed, A.S., Akkurt, N., and Torun, L., 2020, Six-armed structures based on benzene ring, synthesis and characterization via Sonogashira coupling, *Indones. J. Chem.*, 20 (3), 705–715.

[15] Plamont, R., Lancia, F., and Ryabchun, A., 2020, Reactive mesogens for ultraviolet-transparent liquid crystal polymer networks, *Liq. Cryst.*, 47 (11), 1569–1581.

[16] Yan, Q., Wei, Z., Lin, P., Cheng, Z., Pu, M., Huang, Z., and Lin, W., 2018, Polymer stabilized cholesteric liquid crystal particles with high thermal stability, *Opt. Mater. Express*, 8 (6), 228–233.

[17] Abderrahmen, A., Romdhane, F.F., Ben Ouada, H., and Gharbi, A., 2008, Investigation of the liquid crystal alignment layer: Effect on electrical properties, *Sci. Technol. Adv. Mater.*, 9 (2), 025001.

[18] Okafor, O., Popoola, A., Popoola, O., and Adeosun, S., 2024, Surface modification of carbon nanotubes and their nanocomposites for fuel cell applications: A review, *AIMS. Mater. Sci.*, 11 (2), 369–414.

[19] Maulana, M.I., Lee, H.Y., Gyan-Barimah, C., Sung, J.H., and Yu, J.S., 2024, Hollow PtCo alloy nanostructures for efficient oxygen reduction electrocatalysis in polymer electrolyte membrane fuel cells, *J. Mater. Chem. A*, 12 (14), 27979–27986.

[20] Afrizal, A., Rahman, A., Hidayati, N., and Iwan, S., 2019, Effect of doped indium tin oxide on bonding and morphology of monomer cholesteryl acrylate, *Asian J. Chem.*, 31 (10), 2327–2330.

[21] Nguyen, H.T.T., Dang, T.T.N., Ha, T.M., and Nguyen, N.T.Y., 2025, Evaluation of the morphology and malachite green absorption capacity of modified electrospun chitosan nanofibers, *Indones. J. Chem.*, 25 (2), 394–403.

[22] Sadej, M., Gojzewski, H., and Andrzejewska, E., 2016, Photocurable polymethacrylate-silica nanocomposites: Correlation between dispersion stability, curing kinetics, morphology and properties, *J. Polym. Res.*, 23 (6), 116.

[23] Yusmaniar, Y., Adi, W.A., Taryana, Y., and Muzaki, R., 2017, Synthesis and characterization of composite UPR/Fe_3O_4 for its use as electromagnetic wave absorber, *IOP Conf. Ser.: Mater. Sci. Eng.*, 196 (1), 012033.

[24] Zakiyah, N., Kusumawati, N., Setiarso, P., Muslim, S., A'yun, Q., and Putri, M.M., 2024, Characterization and application of natural photosensitizer and poly(vinylidene fluoride) nanofiber membranes-based electrolytes in DSSC, *Indones. J. Chem.*, 24 (3), 701–714.

[25] Khomein, P., Ketelaars, W., Lap, T., and Liu, G., 2021, Sulfonated aromatic polymer as a future proton exchange membrane: A review of sulfonation and crosslinking methods, *Renewable Sustainable Energy Rev.*, 137, 110471.

[26] Achukwu, E.O., Owen, M.M., Bin Shuib, S., Umar, A., Abdulmalik, A.O., Danladi, A., Dauda, B.M., Romli, A.Z., Ishiaku, U.S., and Md Hazizan, A., 2023, Effect of reprocessing on the service life properties of glass fiber-reinforced in-house polypropylene waste composites, *Adv. Manuf.: Polym. Compos. Sci.*, 9 (1), 2195317.

[27] Ahmed, M.B., Nofal, M.M., Aziz, S.B., Al-Saeedi, S.I., Brza, M.A., Dannoun, E.M.A., and Murad, A.R., 2022, The study of ion transport parameters associated with dissociated cation using EIS model in solid polymer electrolytes (SPEs) based on PVA host polymer: XRD, FTIR, and dielectric properties, *Arabian J. Chem.*, 15, 104196.

[28] He, X.Z., Gao, Y.F., Zheng, J.J., Li, X.Y., Meng, F.B., and Hu, J.S., 2016, Chiral photosensitive side-chain liquid crystalline polymers—synthesis and characterization, *Colloid Polym. Sci.*, 294 (11), 1823–1832.

[29] Orhan, M.F., Saka, K., and Yousuf, M., 2022, Design and optimization of fuel cells: A case study on polymer electrolyte membrane fuel cell power systems for portable applications, *Adv. Polym. Technol.*, 2022 (1), 6568456.

[30] Chen, X.Y., Xiao, A., and Rodrigue, D., 2022, Polymer based membranes for propylene/propane separation: CMS, MOF and polymer electrolyte membranes, *AIMS Mater. Sci.*, 9 (2), 184–213.

[31] Poinern, G.E.J., Ali, N., Le, X., and Fawcett, D., 2014, Nano-hardness and elastic modulus of anodic aluminium oxide based poly(2-hydroxyethylmethacrylate) composite membranes, *AIMS Mater. Sci.*, 1 (3), 159–173.

[32] Lu, C., Xiao, H., and Chen, X., 2021, MOFs/PVA hybrid membranes with enhanced mechanical and ion-conductive properties, *e-Polym.*, 21 (1), 160–165.

[33] Li, W., Chang, Z., Lin, L., and Xu, X., 2020, Effect of montmorillonite on PEBAX®1074-based mixed matrix membranes to be used in humidifiers in proton exchange membrane fuel cells, *e-Polym.*, 20 (1), 171–184.

[34] Mohammadi, M., Alirezapour, F., and Khanmohammadi, A., 2024, Adsorption of transition metal cations (Cr^{2+}, Mn^{2+}, Fe^{2+}, Cu^{+}, Ag^{+} and Au^{+}) on boron nitride nanotube: Structural analysis and electronic properties, *Adv. J. Chem., Sect. A*, 7 (4), 355–373.

[35] Li, G., Zhu, D., Jia, W., and Zhang, F., 2021, Analysis of the aging mechanism and life evaluation of elastomers in simulated proton exchange membrane fuel cell environments, *e-Polym.*, 21 (1), 921–929.

[36] Elerian, A.F., Mohamed, A.A., Elnaggar, E.M., Abdel-Naeem, G., and Abu-Saied, M.A., 2024, Investigation on sulfonated PVC/polymethyl methacrylate (PMMA)/polystyrene sulfonate (PSS) polymer blends as proton-conducting membrane, *Polym. Bull.*, 81 (18), 17177–17212.

[37] Jiao, K., Xuan, J., Du, Q., Bao, Z., Xie, B., Wang, B., Zhao, Y., Fan, L., Wang, H., Hou, Z., Huo, S., Brandon, N.P., Yin, Y., and Guiver, M.D., 2021, Designing the next generation of proton-exchange membrane fuel cells, *Nature*, 595 (7867), 361–369.

[38] Chiriaev, S., Madsen, N.D., Rubahn, H.G., and Andersen, S.M., 2017, Helium ion microscopy of proton exchange membrane fuel cell electrode structures, *AIMS Mater. Sci.*, 4 (6), 1289–1304.

[39] Highgate, D.J., 2016, Method for producing a membrane electrode including forming the membrane *in situ*, US Patent No. 9447217, U.S. Patent and Trademark Office, Washington, DC, US.

[40] Thomassin, J.M., Pagnoulle, C., Bizzari, D., Caldarella, G., Germain, A., and Jérôme, R., 2004, Nafion-layered silicate nanocomposite membrane for fuel cell application, *e-Polym.*, 4 (1), 018.